

# Molecular Hydrogen Fluorescence in the Eridanus Superbubble

K. Ryu<sup>1</sup>, K. W. Min<sup>1</sup>, J. W. Park<sup>1</sup>, D. H. Lee<sup>2</sup>, W. Han<sup>2</sup>, U. W. Nam<sup>2</sup>, J. H. Park<sup>2</sup>,  
J. Edelstein<sup>3</sup>, E. J. Korpela<sup>3</sup>, K. Nishikida<sup>3</sup>, E. F. van Dishoeck<sup>4</sup>

ksryu@satrec.kaist.ac.kr

## ABSTRACT

The first FUV ( $\lambda\lambda$  1350–1750Å) spectral imaging observations of the Eridanus superbubble, obtained with the *SPEAR/FIMS* mission, have revealed distinct fluorescent emission from molecular hydrogen. In this study, the observed emission features were compared with those from a photo-dissociation region model with assumed illuminating stellar fields. The result showed rather high line ratios of  $I_{1580}/I_{1610}$ , which may imply the existence of high-temperature molecular clouds in the region. The  $H_2$  fluorescence intensity showed a proportional correlation with  $H\text{-}\alpha$  emission, indicating that the fluorescence and the recombination emission have similar physical origins.

*Subject headings:* ISM: molecules — ISM: supernova remnants — ultraviolet: ISM

## 1. Introduction

The Eridanus region contains a large nearby interstellar superbubble. This region was discovered as an extended  $15^\circ$  X-ray ‘hot spot’ (Williamson et al. 1974; Naranan et al. 1976). Subsequently, the Eridanus Loop was identified as an expanding shell of  $H\text{ I}$  by Heiles (1976) and was extensively imaged in  $H\text{-}\alpha$  emission (Reynolds et al. 1998; Boumis et al. 2001), revealing a large filamentary shell structure. Reynolds and Ogden (1979) argued that Barnard’s Loop and the Eridanus shell were both created by one or more supernovae in the Orion OB association and were maintained by the intense stellar winds and ionizing radiation from those stars. *ROSAT* observations (Snowden et al. 1995) support the idea that the huge interstellar cavity is filled with several-million-degree gas. Surveys of CO (Magnani, Blitz, and Mundy 1985; Aoyama et al. 2002) show that the cavity is bounded in part by molecular gas. The CO clouds generally coincide with  $H\text{ I}$  filaments; however, on a smaller scale, the clouds are located where  $H\text{ I}$  is weak within the filament. In the FUV spectral range, early (Murthy et al. 1993) and improved (Kregenow et al.

---

<sup>1</sup>Korea Advanced Institute of Science and Technology, 305-701, Daejeon, Korea

<sup>2</sup>Korea Astronomy and Space Science Institute, 305-348, Daejeon, Korea

<sup>3</sup>Space Sciences Laboratory, University of California, Berkeley, CA 94720

<sup>4</sup>Sterrewacht Leiden, Postbus 9513, 2300 RA LEIDEN, The Netherlands

2006) spectral observations of diffuse emission from the Eridanus Loop over limited angular fields show that gas at intermediate temperatures,  $T \sim 10^5 \text{ K}$ , exists between the hot superbubble interior and the surrounding material.

We present the first FUV spectral imaging observations of the entire Eridanus Loop. The data were obtained with the Spectroscopy of Plasma Emission from Astrophysical Radiation (*SPEAR*), also known as the Far-ultraviolet Imaging Spectrograph (*FIMS*). These *SPEAR* data show  $\text{H}_2$  fluorescent emission throughout the Eridanus Loop field and provide new insights into the geometry and physical conditions of the molecular environment around this superbubble.

## 2. Observations and Data Reduction

The Eridanus region was observed with *SPEAR*, the main payload of the Korean satellite, STSAT-1, which was launched on September 27, 2003. *SPEAR* is a dual-channel FUV imaging spectrograph (S channel 900–1150Å, L channel 1350–1750Å,  $\lambda/\Delta\lambda \sim 550$ , where  $\Delta\lambda$  refers to the half energy width) with a large field of view (S:  $4.0^\circ \times 4.6'$ , L:  $7.5^\circ \times 4.3'$ , angular resolution  $\sim 10'$ ) optimized for the observation of diffuse emissions. See Edelstein et al. (2006) for an overview of the instrument, mission, and data analysis.

The region bounded by  $\alpha = 2^{\text{h}}30^{\text{m}}$  and  $5^{\text{h}}30^{\text{m}}$ , and  $\delta = +13^\circ$  and  $-23^\circ$ , covering most of the constellations Orion and Eridanus, was observed using more than 16 ks of exposure taken between 26 December 2003 and 26 January 2004. The observation geometry is shown in Figure 1, along with an H- $\alpha$  survey map. The H- $\alpha$  features most prominent around the Eridanus supershell are Barnard’s Loop, the I Orion O-association molecular cloud complex, the H II region surrounding  $\lambda$  Ori centered at  $5^{\text{h}}32^{\text{m}}, +9^\circ50^{\text{m}}$ , and H- $\alpha$  filamentary structures. Barnard’s loop and the  $\lambda$  Ori region were excluded from the *SPEAR* observation to avoid excessive count rates. For the ensuing data analysis, the region was divided, based on the H- $\alpha$  emission features, into subregions labeled as 1 through 6 (See Figure 1).

We identified bright stars in our observations by examining an FUV sky intensity map, created by accumulating photons and exposure into  $2'$  sky bins. Stars were identified by matching features, within  $15'$ , to the position of UV bright stars in the Tycho-2 catalog (Wright et al. 2003). Photons within  $30'$  of the identified stars were removed from the data set to obtain the residual diffuse emission and to minimize stellar contamination. After excluding the contributions of UV bright stars,  $3.0 \times 10^5$  of  $8.8 \times 10^5$  detected photons remained. These photons were accumulated, for each subregion, into spectra that were binned to  $2\text{\AA}$ , shown in Figure 2(a)–(f), along with the noise levels per spectral bin. An inherent detector background of  $\sim 0.013$  counts/s/Å was measured during interleaved shutter-closed periods and was subtracted from these spectra.

### 3. Spectrum Analysis

The Eridanus 1350Å–1630Å spectra show emission features that correspond to the H<sub>2</sub> fluorescence predictions of Sternberg (1989), notably the prominent bands near 1605Å. Other prominent features were identified with atomic lines such as C IV at 1550Å and Si II at 1530Å (See Kregenow et al. (2006) for a discussion of atomic emission in the Eridanus Loop.). To investigate the physical conditions of the H<sub>2</sub>, a photo dissociation region (PDR) radiation code (Black and van Dishoeck 1987) was used to generate a model FUV spectrum. The continuum level was taken to be a linear function of wavelength, and the sensitivity of the fitting while varying the slope and y-intercept of the continuum was investigated based on the  $\chi^2$  minimization method. The fit models for each subregion are shown in Figure 2.

There are several physical parameters which affect the resultant spectrum: cloud density, excitation temperature, total hydrogen molecule column density, and radiation field; we varied only the excitation temperature in our model with other parameters fixed. For example, ultraviolet fluorescent emission of H<sub>2</sub> is produced following the absorption of photons in the Lyman (B  $^1\Sigma_u^+$  – X  $^1\Sigma_g^+$ ) and Werner (C  $^1\Pi_u$  – X  $^1\Sigma_g^+$ ) bands. Hence, the stars in the I Orion OB association were considered as the likely and dominant source of H<sub>2</sub> emission. The total radiation field from the most luminous stars of the I Orion association (Reynolds and Ogden 1979) accounts for the presumed radiation field scale factor (Habing 1968) of  $\chi \sim 1.9$ , assuming that the distance from the association is  $\sim 200$  pc and there is no extinction. Heiles, Haffner, and Reynolds (1999) estimated the electron volume density,  $n_e$ , of the ionized gas in the Eridanus superbubble to be  $0.8 \text{ cm}^{-3}$ , which corresponds to the thermal pressure,  $p/k \sim 1.5 \times 10^4 \text{ cm}^{-3}\text{K}$ , in the ionized gas. The density of the neutral gas was adjusted to have the equilibrium thermal pressure,  $p/k \sim 1.5 \times 10^4 \text{ cm}^{-3}\text{K}$ , according to the excitation temperature, which is used as a parameter in our model. The fractional abundance of H<sub>2</sub>, defined as  $\langle f \rangle = 2\langle n(\text{H}_2) \rangle / [2\langle n(\text{H}_2) \rangle + \langle n(\text{H I}) \rangle]$ , was assumed to have an average value of 0.17, as obtained from the *Copernicus* observations (Savage et al. 1977). The color temperature of the incident radiation was assumed to be  $3 \times 10^4 \text{ K}$ .

With these parameters fixed, the molecular cloud excitation temperature was varied to investigate the sensitivity of the model spectrum compared to the observed data. The model spectrum was scaled to match the average observed intensity over the 1350–1650Å spectral region, where H<sub>2</sub> emission was apparent in both the model and the data. The 1356Å airglow line did not appear in the observed spectrum. The sensitivity of the  $\chi^2$  value to the parameters comes from the relative intensity variations of each vibrational transition band, which are governed by the distribution of H<sub>2</sub> among the vibrational excitation states in the electronic ground state (X  $^1\Sigma_g^+$ ). For example, the intensity ratio,  $I_{1580}/I_{1610}$ , increases monotonically from 0.65 to 0.8 as the excitation temperature increases to 1,000 K, according to our model. Thus, a unique excitation temperature can be determined if the line ratios are measured.

The results for each subregion, the maximum fluorescent emission intensity,  $I_{\text{max H}_2}$ , the continuum intensity  $I_{\text{cont}}$ , and the intensity ratio,  $I_{1580}/I_{1610}$ , are listed in Table 1. The model spectra

with  $T_{\text{ex}} = 50$  K and  $T_{\text{ex}} = 1,000$  K are plotted for Region 4 in Figure 2(g), with the observed spectrum. As can be seen in the figure, most of the lines in the spectral range are identified as Lyman bound-bound transitions (BX  $v' - v''$ ), where  $v'$  and  $v''$  represent the vibrational excitation of a hydrogen molecule at each respective excitation state. The observed spectrum best fits with a cloud excitation temperature of 1,000 K, with  $\chi^2_{\nu} = 2.2$ , though the signal-to-noise ratio of our observation was not sufficient to discriminate the excitation temperature accurately.

#### 4. Discussion

Our detection of  $\text{H}_2$  fluorescence in Eridanus is consistent with previous observations in other locations in that fluorescence is found where  $\text{H}_2$  is exposed to a strong UV radiation field. The correlations among the subregions' fluorescent emission intensity, the  $\text{H}\alpha$  emission intensity, and the color excess value are shown in Figure 3. The  $\text{H}_2$  fluorescence intensity shows a strong correlation with both the  $\text{H}\alpha$  emission intensity and the color excess. This suggests that the  $\text{H}\alpha$  emission and hydrogen molecular fluorescence have similar physical origins and are governed globally by a strong and similar UV radiation field, likely arising from the I Orion OB association. We expect that the  $\text{H}_2$  abundance is proportional to that of both hydrogen atoms and dust particles, since dust particles are known as the main birth place of  $\text{H}_2$  in the interstellar medium.

The most conspicuous features in the  $\text{H}\alpha$  emission map shown in Figure 1, are the filamentary structures elongated along  $\alpha = 4^{\text{h}}$  (Arc A; Region 3) and  $\alpha = 3^{\text{h}}20^{\text{m}}$  (Arc B; Region 5). It appears from Figure 3(a) and (b), and from Figure 1, that UV photons from the Orion OB association undergo extinction by the Arc A and Arc B filaments, since Region 6 shows relatively low  $\text{H}\alpha$  and  $\text{H}_2$  fluorescence, while having a color excess value comparable to those of Region 1, 2, and 5. The  $\text{H}_2$  fluorescent emission from Region 5 (Arc B) is relatively high among regions with comparable dust extinction (Regions 2 and 6), and it is similar to that of Region 4, even though the dust extinction for Region 4 is higher and the line-of-sight distance to the I Orion OB FUV sources is likely smaller. This observation can be explained if the gas in Region 3 (Arc A) is not in the line of sight that extends from the radiation source (the I Orion OB association) to the gas in Region 5 (Arc B), i.e., the distances to Arcs A and B are different and the Eridanus shell structure is open from the I Orion to Arc B. This geometry is consistent with the considerations of Boumis et al. (2001) and Welsh, Sallmen, and Jelinsky (2005) in that both studies argue that Arcs A and B are part of a complex of individual shells viewed along the same line of sight but at different distances (Arc A  $>500\text{pc}$ , Arc B  $\sim 150\text{pc}$ ). The observational results do not rule out Reynolds and Ogden's (1979) description, in that the both Arc A and Arc B can still be exposed to the radiation from the I Orion OB association that causes the  $\text{H}_2$  fluorescent emission.

The FUV continuum intensity does not show a strong correlation with  $\text{H}\alpha$  emission or  $\text{H}_2$  fluorescent emission intensities (See Table 1). Instead, the continuum intensity seems closely tied to the geometry of the region. The strong continuum of Region 1 can be attributed to the proximity of Region 1 to the radiation source. Region 3 is remarkable in that it shows both a strong continuum

intensity and a strong  $\text{H}_2$  fluorescent emission intensity.

The observationally derived shell expansion velocity of the Eridanus region, of between 15 and 23  $\text{km s}^{-1}$  (Heiles 1976; Reynolds and Ogden 1979) is consistent with the survival of the  $\text{H}_2$  in the Eridanus region. The observed  $I_{1580}/I_{1610}$  value suggests the existence of high-temperature molecular gas in the region. According to Draine, Roberge, and Dalgarno (1983), when an interstellar shock with  $v_s = 25 \text{ km/s}$  is running into molecular gas with a density of  $n = 1 \times 10^2 \text{ cm}^{-2}$ , the region in which the gas temperature exceeds 200 K will extend only  $2 \times 10^{16} \text{ cm}$ , implying that interstellar shocks are not good at producing large column densities of warm gas. An alternative explanation, for the heating of molecular gas, might be selective UV excitation by UV lines radiated by the hot gas in the bubble, or it may be that other heating mechanisms are able to raise the gas temperature where UV pumping of the  $\text{H}_2$  is taking place. Further studies are needed to clarify the contribution and role of UV radiation, supernova shocks, and other possible heating mechanisms.

In summary, we have presented the first detection of  $\text{H}_2$  fluorescence in the Eridanus region. The fluorescence emission features, with a PDR spectrum prediction model, imply the possible existence of molecular gas with an excitation temperature as high as 1,000 K, which is about an order of magnitude higher than excitation temperatures generally found for molecular gases in the Galactic disk (Savage et al. 1977). We note that high-excitation temperature  $\text{H}_2$  has also been detected in high-velocity shocked gas associated with the Monoceros Loop (Welsh, Rachford, and Tumlinson 2002) and in a galactic translucent cloud (Snow et al. 2000). The observed spectrum of the  $\text{H}_2$  fluorescence in the Eridanus region is different in that a substantial column density of  $\text{H}_2$  ( $\sim 1.0 \times 10^{20} \text{ cm}^{-2}$ ) is required to produce the observed fluorescence. Thus, most of the  $\text{H}_2$  undergoing photon pumping must have a high rotational temperature, if collisional excitation is to account for the observed fluorescent feature ratios. A more rigorous observation and model study are expected to reveal the physical conditions of the molecular gas in the Eridanus supershell.

*SPEAR/FIMS* is a joint project of KASSI, KAIST (Korea) and U.C., Berkeley (USA) and is funded by the Korea MOST and NASA (Grant no. NAG5-5355).

## REFERENCES

- Aoyama, H., Mizuno, N., Onishi, T., Mizuno, A., & Fukui, Y. 2002, Proc. of APRM, 125
- Black, J. H., & van Dishoeck E. F. 1987, ApJ, 322, 412
- Boumis, P., Dickinson, C., Meaburn, J. and others 2001, MNRAS, 320, 61
- Draine, B. T., Roberge, W. G., and Dalgarno, A. 1983, ApJ, 264, 485
- Edelstein, J., Korpela, E. J. Adolfo, J. and others 2006, ApJ, this issue
- Finkbeiner, D. P. 2002, ApJS, 146, 415

- Habing, H. J. 1968, *Bull. Astr. Inst. Netherlands*, 19, 90
- Heiles, C. 1976, *ApJ*, 208, L137
- Heiles, C., Haffner, L. M., and Reynolds, R. J. 1999, in ASP Conf. Ser. 168, *New Perspectives on the Interstellar Medium*, ed. A. R. Taylor, T. L. Landecker, and G. Joncas (San Francisco: ASP), 211
- Kregenow, J., Edelstein, J., Korpela, E. J. and others 2006, *ApJ*, this issue
- Lynds, B. T. 1962, *ApJS*, 7, 1
- Magnani, L., Blitz, L., and Mundy, L. 1985, *ApJ*, 295, 402
- Murthy, J., Im, M., Henry, R. C., and Holberg, J. B. 1993, *ApJ*, 419, 739
- Naranan, S., Shulman, S., Friedman, and Fritz, G. 1976, *ApJ*, 208, 718
- Reynolds, R. J., and Ogden, P. M. 1979, *ApJ*, 229, 942
- Reynolds, R. J., Tufte, S. L., Haffner, L. M., Jaehnig, K., & Percival, J. W. 1998, *Publ. Astron. Soc. Aust.*, 15, 14
- Savage, B. D., Bohlin, R. C., Drake, J. F., and Budich, W. 1977, *ApJ*, 216, 291
- Snow, T. P., Rachford, B. L., Tumlinson, J. and others 2000, *ApJ*, 538, L65
- Snowden, S. L., Burrows, D. N., Sanders, W. T., Aschenbach, B., and Pfeffermann, E. 1995, *ApJ*, 439, 404
- Sternberg, A. 1989, *ApJ*, 347, 863
- Welsh, B. Y., Rachford, B. L., and Tumlinson, J. 2002, *A&A*, 381, 566
- Welsh, B. Y., Sallmen, S., and Jelinsky, S. 2005, *A&A*, accepted
- Williamson, F. O., Sanders, W. T., Kraushaar, W. L., McCammon, D., Borken, R., and Bunner, A. N. 1974, *ApJ*, 193, L133
- Wright, C. O., Egan, M. P., Kraemer, K. E., and Price, S. D. 2003, *AJ*, 125, 359

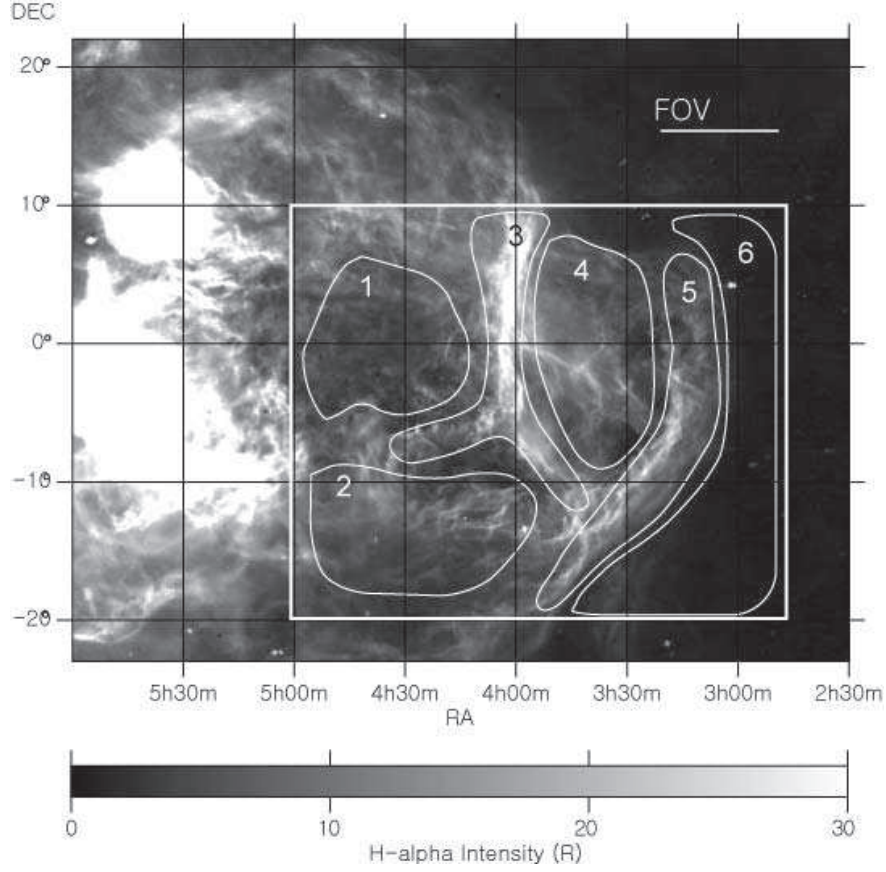


Fig. 1.— Observation geometry of the Eridanus region marked over an H- $\alpha$  map. The marked rectangular region was observed with *SPEAR*. The observed region was divided into subregions, labeled 1 through 6, for spectral analysis and interpretation. The thick solid line, in the upper right corner, designates the *SPEAR* field of view.

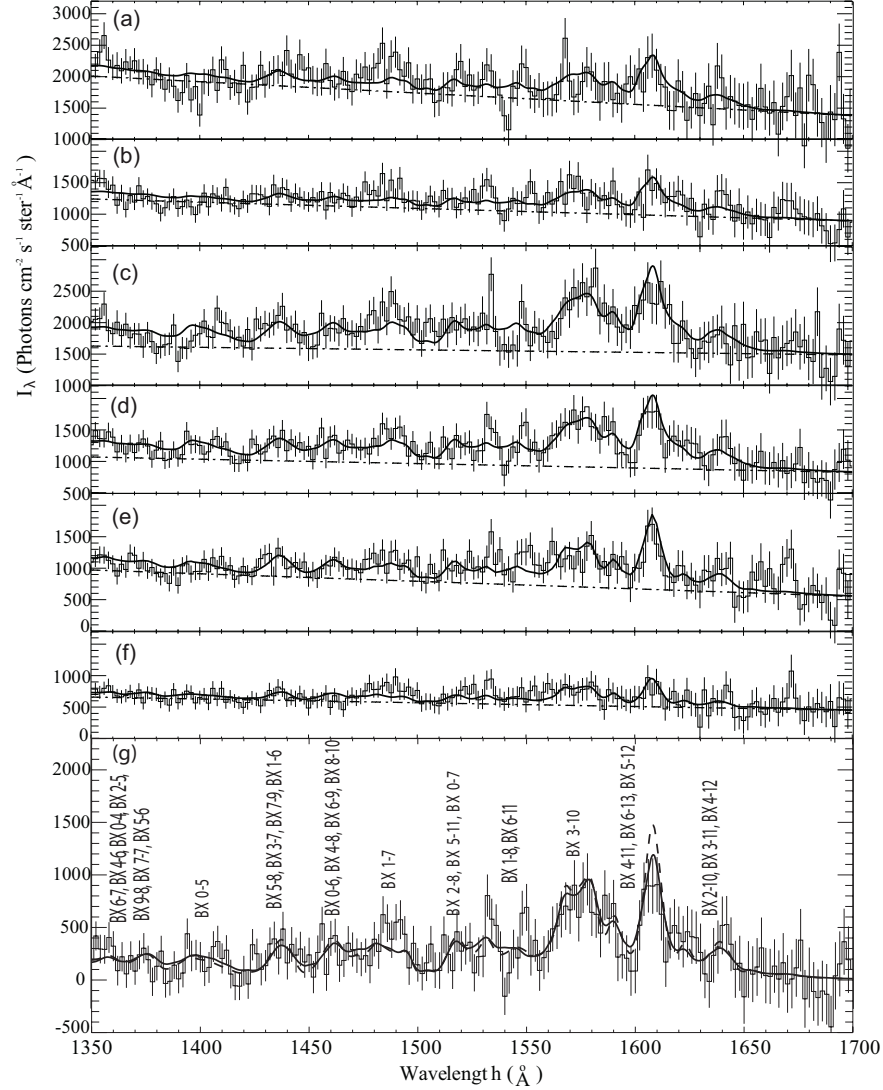


Fig. 2.— *SPEAR* FUV diffuse spectra of Eridanus subregions 1 - 6, shown in panels (a) - (f). The histogram is the observed spectrum. The thick solid line and the dashed line are the best-fit model of  $\text{H}_2$  fluorescent emission and continuum intensities, respectively. The noise levels are shown as vertical bars. (g) The continuum subtracted diffuse spectrum of Region 4 with different  $\text{H}_2$  model parameters. The dashed line represents for  $T_{\text{ex}} = 50 \text{ K}$ . The solid line represents for  $T_{\text{ex}} = 1,000 \text{ K}$ . The legends, marked as BX  $v' - v''$ , show the positions of Lyman bound-bound transitions.

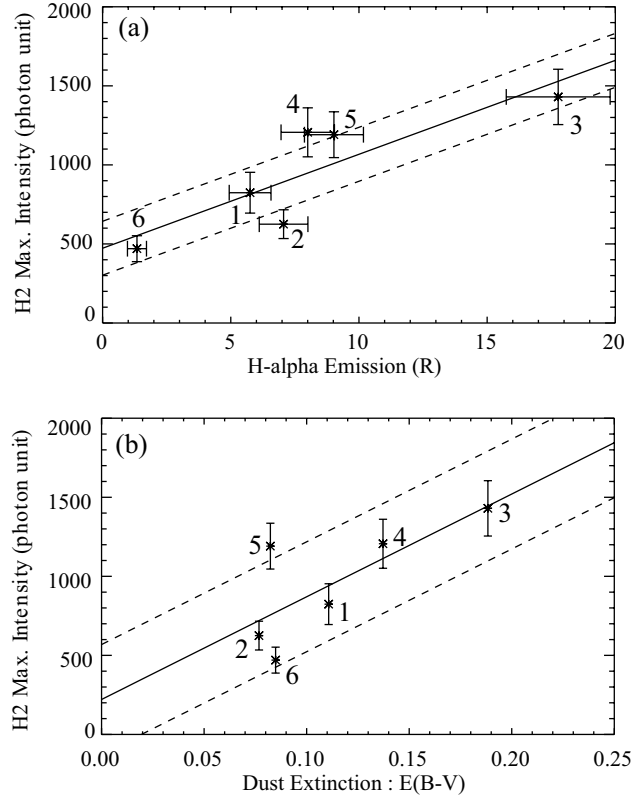


Fig. 3.— Comparison of the H<sub>2</sub> fluorescent emission intensity (asterisks) for the subregions with (a) the H- $\alpha$  emission intensity and (b) the color excesses (Finkbeiner 2002). The measurement error ranges are represented with error bars. The solid lines are the best linear fits, and the dashed lines show the 1  $\sigma$  uncertainty in  $b$ , in the linear fit  $y = ax + b$ .

Table 1: Observational results for regions in Eridanus.

Region	$I_{cont.}^a$	$I_{max.H_2}^b$	$\chi_\nu^2$	$I_{1580}/I_{1610}^c$	$H-\alpha(R)^d$	$E(B-V)^e$
1	$1590 \pm 165$	$825 \pm 130$	2.1	$0.8 \pm 0.4$	$5.7 \pm 0.8$	0.11
2	$1065 \pm 110$	$625 \pm 90$	2.3	$0.5 \pm 0.3$	$7.0 \pm 0.9$	0.08
3	$1555 \pm 160$	$1430 \pm 175$	2.0	$1.2 \pm 0.35$	$17.7 \pm 2.0$	0.19
4	$915 \pm 100$	$1205 \pm 155$	2.2	$0.9 \pm 0.25$	$8.0 \pm 1.0$	0.14
5	$720 \pm 80$	$1190 \pm 145$	3.8	$0.85 \pm 0.25$	$9.0 \pm 1.2$	0.08
6	$520 \pm 60$	$470 \pm 80$	2.9	$1.2 \pm 0.6$	$1.3 \pm 0.4$	0.08

<sup>a,b</sup>The intensity of the continuum at 1525Å,  $I_{cont}$ , and the maximum H<sub>2</sub> fluorescent emission from 1600 to 1620Å,  $I_{max.H_2}$ , in units of photons/cm<sup>2</sup>/sr/Å/s.

<sup>c</sup>The line ratio,  $I_{1580}/I_{1610}$ , is estimated by summing 3 spectral bins (6Å interval), centered at 1580Å and 1610Å.

<sup>d</sup>The H-α intensity values from Reynolds et al. (1998)

<sup>e</sup>The color excess values, E(B-V) from Finkbeiner (2002).